



Nanoporous molybdenum carbide wires as an active electrocatalyst towards the oxygen reduction reaction

Journal:	<i>Physical Chemistry Chemical Physics</i>
Manuscript ID:	CP-ART-11-2013-054754.R1
Article Type:	Paper
Date Submitted by the Author:	26-Jan-2014
Complete List of Authors:	Liao, Lei; Fudan University, Department of Chemistry Bian, XiaoJun; Fudan University, Department of Chemistry Xiao, Jingjing; Fudan university, Chemistry of department Liu, Baohong; Fudan University, Department of Chemistry; Scanlon, Micheal; EPFL-SB-ISIC-LEPA, Girault, Hubert H; EPFL-SB-ISIC-LEPA,

Nanoporous molybdenum carbide wires as an active electrocatalyst towards the oxygen reduction reaction

Lei Liao,^{a,b} Xiaojun Bian,^a Jingjing Xiao,^a Baohong Liu,^{a,*} Micheál D. Scanlon^b and Hubert H. Girault^{b,*}

^aDepartment of Chemistry, State Key Lab of Molecular Engineering of Polymers and Collaborative Innovation Center of Chemistry for Energy Materials, Fudan University, Shanghai 200433, P. R. China; Email: bhliu@fudan.edu.cn;

^bLaboratoire d'Electrochimie Physique et Analytique, École Polytechnique Fédérale de Lausanne, CH-1015 Lausanne, Switzerland; Email: hubert.girault@epfl.ch.

Abstract

A non-precious metal electrocatalyst has been developed for the oxygen reduction reaction based on nanoporous molybdenum carbide (nano-Mo₂C) wires through a facile calcination of sub-nanometer periodic organic-inorganic hybrid nanowires. The highly dispersed Mo₂C wires were composed of 10-15 nm nanocrystals with size of 3.3 nm. The properties of nano-Mo₂C wires were characterized by scanning electron microscopy, transmission electron microscopy, X-ray diffraction and N₂ adsorption/desorption porosimetry. The highly active surface area and enriched nanoporosity for nano-Mo₂C wires are unique features that make them a high-performance electrocatalyst for oxygen reduction in an alkaline medium. The

electrocatalysis and reaction kinetics results show that nano-Mo₂C-based materials can be developed as new catalysts with high activity at low cost for electrochemical conversion applications.

Keywords: Electrocatalyst, molybdenum carbide, nanomaterials, oxygen reduction reaction

1. Introduction

The field of energy conversion and storage has been the subject of increased efforts in recent years. In particular the oxygen reduction reaction (ORR) at the anode in fuel cells has attracted considerable attention.¹⁻³ Platinum (Pt) and its alloys are the most effective electrocatalysts for the ORR, however, as Pt-based catalysts are expensive and of low abundance, this limits their large-scale applicability in many fields.⁴⁻⁶ The development of efficient ORR catalysts that can replicate the catalytic activity of Pt-based materials remains challenging and many efforts have been in this direction. Non-precious metals and metal-free materials including non-pyrolyzed and pyrolyzed transition metal nitrogen-containing complexes,⁷ transition metal chalcogenides,⁸ metal oxides^{9, 10} /carbides¹¹ /nitrides,¹² N-doped graphene¹³ or mesoporous carbon nitrides,¹⁴ and enzymatic compounds¹⁵ have been actively pursued as alternative electrocatalysts. Among these candidates, pyrolyzed transition metal nitrogen-containing complexes are considered the most promising ORR catalysts because they have demonstrated ORR activity and stability close to

of commercially available Pt/C catalysts. Although great progress has been achieved in this field, it is still challenging but desirable to develop efficient catalysts for the ORR. Transition metal carbides often display electronic and catalytic properties that are similar to Pt-group metals.¹⁶ Following the pioneering work of Hu *et al.*,¹⁷ our groups have demonstrated that molybdenum carbides are active catalysts for the hydrogen evolution reactions both on modified electrodes and at soft interfaces.¹⁸⁻²⁰ Their attractive physicochemical properties, originating from the unique metal-carbon chemical bonds and noble-metal-like d-state density around the Fermi level, of stability, mechanical hardness and high catalytic performance in hydrocarbon conversion has led to them being carefully scrutinized as promising ORR catalysts.²¹

Herein, we propose a nano-sized Mo₂C wire that acts as an advanced electrocatalyst towards the oxygen reduction reaction. To realize this purpose, the nanoporous molybdenum carbide wires were prepared through a facile calcination of sub-nanometer periodic organic-inorganic hybrid nanowires and successfully demonstrate a high ORR performance. The unique features of such Mo₂C wires, including high active surface areas and enriched nanoporosity, lead not only to more exposed edge sites for catalysis but also facilitate highly efficient dispersion in a reaction solution. Both of these factors lead to a high electrocatalytic activity towards ORR and stability in an alkaline medium. As the structure of these nano-Mo₂C wires is different to that of commercial catalysts, our insights may lead to new theoretical and experimental investigations regarding molybdenum-containing ORR catalysts.

2. Experimental

Reagents

Ammonium heptamolybdate ((NH₄)₆Mo₇O₂₄•4H₂O), aniline, commercial Mo₂C, Vulcan carbon and Nafion® perfluorinated ion-exchange resin solution (5% w/w), Pt/C (10 wt. % platinum on Vulcan carbon) were purchased from Sigma-Aldrich. Other reagents were obtained from the Shanghai Chemical Plant. Ethanol, methanol and KOH were obtained from the Shanghai Chemical Plant. All aqueous solutions were prepared with ultra pure water.

Synthesis of nano-Mo₂C wires

Nanoporous Mo₂C wires were prepared according to our previous report with some modifications.¹⁸ The precursor of Mo₃O₁₀(C₆H₈N)₂•2H₂O was first synthesized through a facile method. Typically, 2.48 g of ammonium heptamolybdate and 3.2 g of aniline were added to 40 mL of distilled water. Next an aqueous solution of 1.0 M HCl was added drop-wise, with magnetic stirring at room temperature, until a white precipitate appeared (the pH was approximately 4 to 5). After stirring at 50 °C for 5 hours, the product was filtered, washed with ethanol and dried at 50 °C for 10 hours. After expelling air for 4 hours at room temperature using argon, the obtained precursor was calcinated at 725 °C for 5 hours under an argon flow to obtain the nano-Mo₂C wire catalyst. Considering that Pt may influence the catalytic results,²⁴ Pt crucibles were not used at any stage during the synthesis processes and, additionally, the porcelain crucible used was never exposed to any Pt metal or Pt containing species.

Characterization

The morphology of nano-Mo₂C wires was characterized by scanning electron microscopy (SEM, Philips XL 30) at 10 keV and transmission electron microscopy (TEM, JEOL JEM-2011 electron microscope) at an acceleration voltage of 200 keV. X-ray diffraction (XRD) patterns were obtained on a Bruker D8 Advance. Nitrogen adsorption/desorption isotherms were collected with the aid of Quantachrome's Quadrasorb SI analyzer at 77 K. Prior to measurements, the samples were degassed at 523 K for 3 hours under vacuum. The Brunauer-Emmett-Teller (BET) method was used to calculate the specific surface area. The pore size distribution was analysed by the thermodynamics-based Barrett-Joyner-Halenda (BJH) method²⁵ with a spherical pore model on the adsorption branch of the isotherms. The total pore volume was calculated from the adsorbed amount at a maximum relative pressure P/P_0 .

Electrochemical measurements

Electrochemical measurements were carried out on a CHI660C electrochemical workstation (CH instruments, Texas, USA). A platinum wire and a saturated calomel electrode (SCE) were used as the counter and reference electrodes, respectively. For rotating disk electrode (RDE) measurements, PINE research instrumentation (USA) was used and a glassy carbon disk electrode (GCE) acted as the working electrode (5 mm diameter). The GCE was modified with 10 μ L of 4 mg/mL nano-Mo₂C wire catalyst suspensions in water and ethanol (w/w = 4:1 containing 80 μ L of 5 wt. % Nafion per mL). The modified GCE was left to dry at room temperature. For

comparison, GCEs were modified with commercial Mo₂C catalysts, Pt/C (10 wt. % platinum on Vulcan carbon, Sigma) and nano-Mo₂C wires physically mixed with Vulcan carbon. Each modified GCE was loaded with an identical amount of Mo₂C (0.21 mg/cm²). For all electrochemical measurements, oxygen saturated 0.1 M KOH aqueous solutions were used as the electrolyte and a flow of oxygen maintained over the electrolyte for the duration of each measurement in order to ensure continuous oxygen saturation. Prior to each measurement, a resistance test was performed and *iR* compensation applied using the CHI software. The electrocatalytic activity of nano-Mo₂C wires towards the ORR was determined by polarization curves using sweep voltammetry (LSV) at a scan rate of 10 mV/s. LSV was performed at various rotation rates from 400 rpm to 2025 rpm. Cyclic voltammograms (CVs) were at a scan rate of 50 mV/s. The working electrode was cycled at least five times for activation in oxygen saturated 0.1 M KOH aqueous solutions before data were collected. During control experiments, CV measurements were also performed under anaerobic conditions by switching to a nitrogen flow through the electrochemical cell. All electrochemical data was collected at room temperature (25 °C), maintained using a thermostatic water bath.

3. Result and discussion

Synthesis and characterization of nano-Mo₂C wires

The nanoporous Mo₂C wires were prepared by calcinating organic-inorganic hybrid Mo₃O₁₀ (C₆H₈N)₂·2H₂O nanowire precursors at 725 °C under an argon flow.¹⁸ The

intercalating amine molecules act as both the reducing agent and the source of carbon this reaction. Fig. 1A depicts a scanning electron microscopy (SEM) image of nano-Mo₂C where the wire-like products of uniform morphology, several micrometers in length and 80-150 nm in width, were observed. The transmission electron microscopy (TEM) images (Fig. 1B) confirmed their highly dispersed morphologies with individual wires. A high-resolution TEM image (Fig. 1C and Fig. 1D) highlights the formation of a crystalline framework composed of 10-15 nm nanocrystallites. The orientation (101) of the Mo₂C nanocrystals agrees with that indicated by the XRD pattern in Fig. 2A, which are confirmed as hexagonal phase (JCPDS: 35-0787). The aggregation of the Mo₂C nanocrystallites inside the wires leads to a BET surface area 53.3 m²/g and a pore size of 3.3 nm in diameter, as confirmed by a N₂ sorption (Fig. 2B).

Electrocatalytic properties toward the ORR

The electrocatalytic properties of commercial Mo₂C and nano-Mo₂C wires were compared with that of both bare and commercial Pt-C (10 wt. % platinum on Vulcan carbon) modified glassy-carbon rotating-disk electrodes (GC-RDE, 5 mm diameter) in oxygen or nitrogen saturated 0.1 M KOH solutions using a three-electrode setup. The same amount of each catalyst by mass (0.21 mg/cm²) was loaded onto each GC-RDE. Polarisation curves of GC-RDEs modified with various catalysts, as noted, are shown in Figs. 3A & B. Firstly, the activity of a bare GC-RDE was substantially less than that of a nano-Mo₂C wires modified GC-RDE (Fig. 3A). The nano-Mo₂C wires showed a

considerably more positive ORR onset potential, (at approximately 0.87 V *vs.* RHE) than both the bare GC-RDE (Fig. 3A) and that modified by commercial Mo₂C (Fig. 3B). Indeed, the onset potential of the nano-Mo₂C wires modified GC-RDE was close to that identified from CV measurements (0.86 V *vs.* RHE, Fig. 3B and Fig. 3C). Meanwhile, the Pt-C catalyst modified GC-RDE showed better catalytic activity with an onset potential of 0.99 V (*vs.* RHE) corroborating the existing literature on this catalyst.^{5,6} In order to confirm the reproducibility of the catalytic responses for each modified GC-RDE, five individual electrodes were tested. An average current density at 0.4 V (*vs.* RHE) of -2.94 mA/cm^2 was obtained at a rotation rate of 1600 rpm. The relative standard deviation was approximately 1.4 % for these measurements, thereby confirming the reproducibility of the catalytic response. Fig. 3C and Fig. 3D present CVs of a nano-Mo₂C wire modified GCE and a Pt-C modified GCE, respectively, in oxygen or nitrogen saturated 0.1 M KOH solutions at a scan rate of 50 mV/s. Featureless voltammetric responses were observed for a nano-Mo₂C wire modified GCE in nitrogen saturated solutions within the studied potential range. In contrast, when the electrolyte solution was saturated with oxygen, the reduction current appeared as a well-defined cathodic peak at 0.76 V (*vs.* RHE), suggesting pronounced electrocatalytic activity of the nano-Mo₂C wire modified GCE for oxygen reduction.

To examine possible crossover effects, we measured the electrocatalytic selectivity of nano-Mo₂C wire modified and Pt-C modified GCEs against the electrooxidation of methanol in oxygen-saturated 0.1 M KOH. For a Pt-C modified GCE in the presence methanol (3.0 M), the obtained CV exhibited one pair of peaks for methanol oxidation,

whereas the cathodic peak for ORR had vanished (Fig. 3D). However, with a nano-Mo₂C wire modified GCE, no noticeable change was observed in the oxygen-reduction current under the same conditions (Fig. 3C). Thus, nano-Mo₂C exhibited high selectivity for the ORR, with a remarkably good ability to avoid crossover effects and outperformed the Pt-C catalyst. Such Mo₂C nanowires may hold promise for use in direct methanol and alkaline fuel cells.

Kinetics and stability study

The reaction kinetics were further studied to gain insights into the role of nano-Mo₂C wires during the ORR electrochemical process. The voltammetric profiles in an oxygen saturated 0.1 M KOH solution showed that the current density was enhanced on increasing the rotation rates (from 400 rpm to 2025 rpm, Fig. 4A). The corresponding Koutecky-Levich plots (J^{-1} vs. $\omega^{-1/2}$) at various electrode potentials exhibited good linearity (Fig. 4B). The kinetic parameters can be analyzed on the basis of the Koutecky-Levich (K-L) equations.²⁶⁻²⁸

$$J^{-1} = J_L^{-1} + J_K^{-1} \quad (1)$$

$$J_L = 0.62nFC_0D^{2/3}\nu^{-1/6}\omega^{1/2} \quad (2)$$

$$J_K = nFkC_0 \quad (3)$$

where J is the current density, J_K and J_L are the kinetic- and diffusion-limiting current densities, ω is the angular velocity of the disk ($\omega = 2\pi N$, N being the rotation frequency), n is the overall number of electrons transferred in oxygen reduction, F is the Faraday constant ($F = 96485$ C/mol), D is the diffusion coefficient of O₂ in 0.1 M

KOH electrolyte ($1.9 \times 10^{-5} \text{ cm}^2/\text{s}$), C_0 is the bulk concentration of O_2 ($1.2 \times 10^{-3} \text{ mol/L}$), ν is the kinetic viscosity of the electrolyte ($0.01 \text{ cm}^2/\text{s}$) and k is the electron transfer rate constant. According to the K-L plots, the average electron transfer n for nano- Mo_2C wires towards the ORR is 3 over the potential range from 0.7 V to V (vs. RHE) and 4 over the potential range from 0.3 V to 0 V (vs. RHE). This suggests that the ORR process at a nano- Mo_2C catalyst is a combination of two-electron and four-electron pathways or a two-step two-electron process with the formation of intermediate HO_2^- ions as indicated by two reduction waves started at $\sim 0.87 \text{ V}$ and $\sim 0.41 \text{ V}$ (vs. RHE), respectively.¹³

Tafel analysis was also performed to gain information about the oxygen adsorption mechanism on nano- Mo_2C wire modified GC-RDEs. Diffusion-corrected Tafel plots were employed to eliminate the impact of diffusion on the adsorption kinetic analysis by plotting the potentials (E) as a function of the absolute values of the kinetic ($|J_k|$) in a semilogarithmic form (Fig. 4C). In the low-overpotential region ($> 0.8 \text{ V}$), where the overall ORR speed is determined by the surface reaction rate on the catalyst, the Tafel slope for nano- Mo_2C wires is $\sim 65 \text{ mV/decade}$ (from 0.87 V to 0.83 V vs. RHE), which is very close to the value for a Pt/C catalyst ($\sim 64 \text{ mV/decade}$).^{29, 30} Additionally, the nano- Mo_2C wires exhibit comparable stability to a Pt-C catalyst in oxygen saturated 0.1 M KOH solutions with 13% decay in ORR activity over 25000 s (Fig. 5). Pt catalysts are known to gradually degrade over time because of the irreversible formation of surface oxides and particle dissolution and aggregation, especially in the alkaline electrolytes used for fuel cells. As the lack of catalyst stability

is one of the major challenges facing alkaline fuel cells, exploring routes to develop more durable catalysts for the ORR in alkaline solutions is a priority.⁹

The precise nature of the catalytic sites for the ORR with Mo₂C-based materials is still a matter of debate. Previously, Vrabel and Hu¹⁷ have shown that the surface of Mo₂C particles are contaminated with molybdenum oxides, such as MoO₃ and MoO₂, prior to electrochemical activation. We have also found this to be the case from preliminary X-ray photoelectron spectroscopy (XPS) of our nano-Mo₂C wires (not shown). In addition, Vrabel and Hu noted that, firstly, the amounts of MoO₃ and MoO₂ greatly diminished after activation by Galvanostatic electrolysis for short periods of time and, secondly, that MoO₂, MoO₃ and Mo metal are not efficient catalysts for the hydrogen evolution reaction (HER).¹⁷ Accordingly, a future perspective of this work will be to perform a more in-depth investigation to determine the precise nature of the true catalytic sites for the ORR after Mo₂C activation, *i.e.*, are they Mo₂C itself, molybdenum oxides or, perhaps, molybdenum oxycarbide species. This work will be predominantly based on in-depth XPS analysis using a custom setup (with extreme care necessary to prevent activated electrode surfaces being re-oxidised by exposure to air) and theoretical approaches using density functional theory (DFT) calculations.

Electrocatalytic properties of a Mo₂C-carbon composite toward the ORR

Moreover, it is known that the morphology and electrical conductivity of catalysts are important factors affecting the electrocatalytic efficiency. Considering that carbon

materials are ideal supports to improve the electrocatalytic activity, here the nano-Mo₂C wires and commercial Vulcan carbon (Mo₂C/carbon) were further physically mixed to modify a GC-RDE. Fig. 6B indicated that the catalytic current density was enhanced compared with that of pure nano-Mo₂C wire catalysts. This could be attributed to the improved conductivity due to the contact of nano-Mo₂C wires with the carbon, which afforded facilitated electron transfer between the Mo₂C/carbon and the electrode.¹⁷ SEM images (Fig. 6A) confirmed the close nature of this interaction highlighting the distribution of the carbon nanoparticles and their attachment to the Mo₂C wires. The LSV curves measured with mixed nano-Mo₂C/carbon catalyst modified GC-RDE at various rotation speeds are presented in Fig. 7A, showing increasing cathodic current at increasing rotation speeds due to improved mass transport at the electrode surface. From the slope of the Koutecky-Levich plots obtained from the data in Fig. 7A, the number of electrons per oxygen molecule in the ORR is calculated to be 3 over the potential range from 0.7 V to 0.4 V (*vs.* RHE) and 4 over the potential range from 0.3 V to 0 V (*vs.* RHE) (Fig. 7B), consistent with the results of nano-Mo₂C wires. Similar catalytic mechanisms may occur in both systems in the present study. This proof-of-concept experiment showed that supporting nano-sized Mo₂C on functional carbon matrices could be expected to improve the electronic conductivity and catalyst dispersibility, thus promoting the electrocatalytic activity by synergetic effects. Future perspectives will focus on *in situ* formation of Mo₂C nanocomposites on various carbon supports as advanced electrocatalysts for oxygen reduction reactions.

4. Conclusions

In conclusion, nanoporous molybdenum carbide wires have been synthesized by a simple, cost-effective and safe approach. The special features of nano-Mo₂C wires are their enriched nanoporosity and large active surface areas that accelerate the interfacial electrochemical reaction, contributing to their potent ORR activity. The resulting nano-Mo₂C wires are shown to be efficient catalysts towards the oxygen reduction reaction showing high electrocatalytic activity, excellent resistance to crossover effects and comparable stability towards the ORR to another well known, but precious metal containing, Pt-C catalyst. Additionally, proof-of-concept results show that the catalytic performance could be further improved through supporting the nanoparticles of Mo₂C on functional carbon materials with synergistic effects, which may open up a new road to advanced catalysts for energy conversion and storage.

Acknowledgement

This work was supported by NSFC 20925517, SKLEAC201101 and Swiss Science Foundation grant 200 021-134 745.

References

- 1 B.C.H. Steele and A. Heinzl, *Nature*, 2001, **414**, 346-352.
- 2 N.S. Lewis and D.G. Nocera, *Proc. Natl. Acad. Sci. U. S. A.*, 2006, **103**, 15729-15735.
- 3 Q. Li, M. C. Henstridge, C. B. McAuley, N. S. Lawrence, R. S. Hartshorne and R. G. Compton, *Phys. Chem. Chem. Phys.* 2013, **15**, 7854-7865.
- 4 A. C. Garcia and E. A. Ticianelli, *Electrochimica Acta*, 2013, **106**, 453-459.
- 5 Y. Li, Y. Li, E. Zhu, T. McLouth, C.-Y. Chiu, X. Huang and Y. Huang, *J. Am. Chem. Soc.*, 2012, **134**, 12326-12329.
- 6 B. Lim, M. Jiang, P.H.C. Camargo, E.C. Cho, J. Tao, X. Lu, Y. Zhu and Y. Xia, *Science*, 2009, **324**, 1302-1305.
- 7 Z. Chen, D. Higgins, A. Yu, L. Zhang and J. Zhang, *Energy Environ. Sci.*, 2011, **4**, 3167-3192.
- 8 M.-R. Gao, J. Jiang and S.-H. Yu, *Small*, 2012, **8**, 13-27.
- 9 Y. Liang, Y. Li, H. Wang, J. Zhou, J. Wang, T. Regier and H. Dai, *Nat Mater.*, 2011, **10**, 780-786.
- 10 Y. Liang, H. Wang, J. Zhou, Y. Li, J. Wang, T. Regier and H. Dai, *J. Am. Chem. Soc.*, 2012, **134**, 3517-3523.
- 11 X. Li, D. Ma, L. Chen and X. Bao, *Catal Lett.*, 2007, **116**, 63-69.
- 12 Y. Li, T. Takata, D. Cha, K. Takanabe, T. Minegishi, J. Kubota and K. Domen, *Adv. Mater.*, 2013, **25**, 125-131.

- 13 B. Zheng, J. Wang, F.-B. Wang and X.-H. Xia, *Electrochem. Commun.*, 2013, **28**, 24-26.
- 14 K. Kwon, Y.J. Sa, J.Y. Cheon and S.H. Joo, *Langmuir*, 2012, **28**, 991-996.
- 15 Y.C. Weng, F.-R.F. Fan and A.J. Bard, *J. Am. Chem. Soc.*, 2005, **127**, 17576-17577.
- 16 S.-H. Jhi, J. Ihm, S.G. Louie and M.L. Cohen, *Nature*, 1999, **399**, 132-134.
- 17 H. Vrubel and X. L. Hu, *Angew. Chem. Int. Ed.*, 2012, **51**, 12703-12706.
- 18 L. Liao, S. Wang, J. Xiao, X. Bian, Y. Zhang, M. D. Scanlon, X. Hu, Y. Tang, B. Liu and H. H. Girault, *Energy Environ. Sci.*, 2014, **7**, 387 - 392.
- 19 X. Bian, M. D. Scanlon, S. Wang, L. Liao, Y. Tang, B. Liu and H. H. Girault, *Chem. Sci.*, 2013, **4**, 3432-3441.
- 20 M. D. Scanlon, X. Bian, H. Vrubel, V. Amstutz, K. Schenk, X. Hu, B. Liu and H. H. Girault, *Phys.Chem. Chem. Phys.*, 2013, **15**, 2847-2857.
- 21 V. G. Pol, S. V. Pol and A. Gedanken, *Eur. J. Inorg. Chem.*, 2009, **2009**, 709-715.
- 22 R. Jäger, P. E. Kasatkin, E. Härk, E. Lust, *Electrochem. Commun.* 2013, **35**, 97-99.
- 23 Q. Gao, C. Zhang, S. Xie, W. Hua, Y. Zhang, N. Ren, H. Xu and Y. Tang, *Chem. Mater.*, 2009, **21**, 5560-5562.
- 24 R. H. Crabtree, *Chem Rev.*, 2012, **112**, 1536-1554.
- 25 E.P. Barrett, L.G. Joyner and P.P. Halenda, *J. Am. Chem. Soc.*, 1951, **73**, 373-380.

26. L. Qu, Y. Liu, J.-B. Baek and L. Dai, *ACS Nano*, 2010, **4**, 1321–1326.
27. W. Chen and S. Chen, *Angew. Chem. Int. Ed.*, 2009, **48**, 4386-4389.
28. A.J. Bard and L.R. Faulkner, *Electrochemical Methods: Fundamentals and Applications*, Wiley, New York, 2001.
29. J. Liang, Y. Zheng, J. Chen, J. Liu, D. Hulicova-Jurcakova, M. Jaroniec and S.Z. Qiao, *Angew. Chem. Int. Ed.*, 2012, **51**, 3892-3896.
30. Z. Chen, Drew Higgins, H. Tao, R.S. Hsu and Z. Chen, *J. Phys. Chem. C*, 2009, **113**, 21008-21013.

Figure captions:

Fig. 1. SEM (A) and TEM (B, C) images of nano-Mo₂C wires. (D) High-resolution TEM image of nano-Mo₂C wires confirming that such wires are composed of nanoparticles.

Fig. 2. (A) XRD pattern and (B) N₂ adsorption/desorption isotherm of nano-Mo₂C wires.

Fig. 3. Polarisation curves of (A) bare and nano-Mo₂C wire modified GC-RDEs and (B) commercial Mo₂C, nano-Mo₂C wire and Pt-C modified GC-RDEs. The LSV experiments were performed with a rotation rate of 1600 rpm, at a scan rate of 10 mV/s, in an oxygen saturated 0.1 M KOH solution. CVs of (C) nano-Mo₂C wires and (D) Pt-C modified GC-RDEs in an oxygen saturated 0.1 M KOH solution, an oxygen saturated 0.1 M KOH solution with the addition of methanol (3.0 M), and a nitrogen saturated 0.1 M KOH solution. Scan rate: 50 mV/s.

Fig. 4. (A) Polarisation curves of a nano-Mo₂C wire modified GC-RDE with various rotation rates at a scan rate of 10 mV/s in an oxygen saturated 0.1 M KOH solution. (B) The Koutecky-Levich plots of J^{-1} versus $\omega^{-1/2}$ deduced from the data of (A) at different potentials. (C) Tafel plots of nano-Mo₂C derived by the mass-transport correction of the corresponding rotating disk electrode data.

Fig. 5. Chronoamperometric response of nano-Mo₂C wires and Pt-C kept at 0.6 V (vs. RHE) in an oxygen saturated 0.1 M KOH solution.

Fig. 6. (A) SEM image of nano-Mo₂C wires physically mixed with Vulcan carbon. (B) Polarisation curves of nano-Mo₂C wires, mixed nano-Mo₂C/carbon catalyst modified GC-RDEs with a rotation rate of 1600 rpm, at a scan rate of 10 mV/s, in an oxygen saturated 0.1 M KOH solution.

Fig. 7. (A) Polarisation curves of mixed nano-Mo₂C/carbon catalyst modified GC-RDE with various rotation rates at a scan rate of 10 mV/s in an oxygen saturated 0.1 M KOH solution. (B) The Koutecky-Levich plots of J^{-1} versus $\omega^{-1/2}$ deduced from the data of (A) at different potentials.

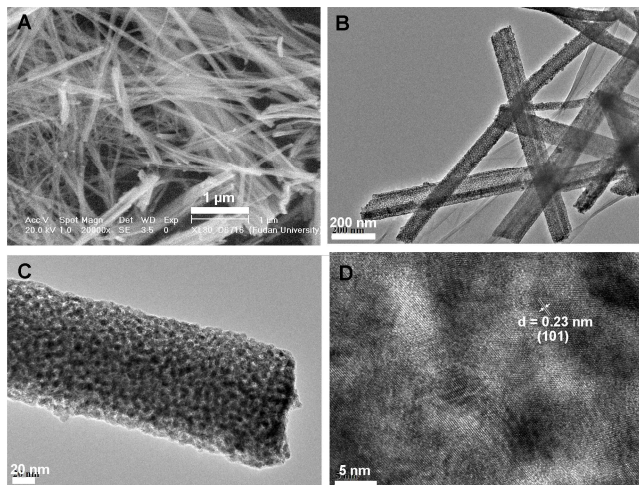


Fig. 1. SEM (A) and TEM (B, C) images of nano-Mo₂C wires. (D) High-resolution TEM image of nano-Mo₂C wires confirmed that such wires are composed of nanoparticles.

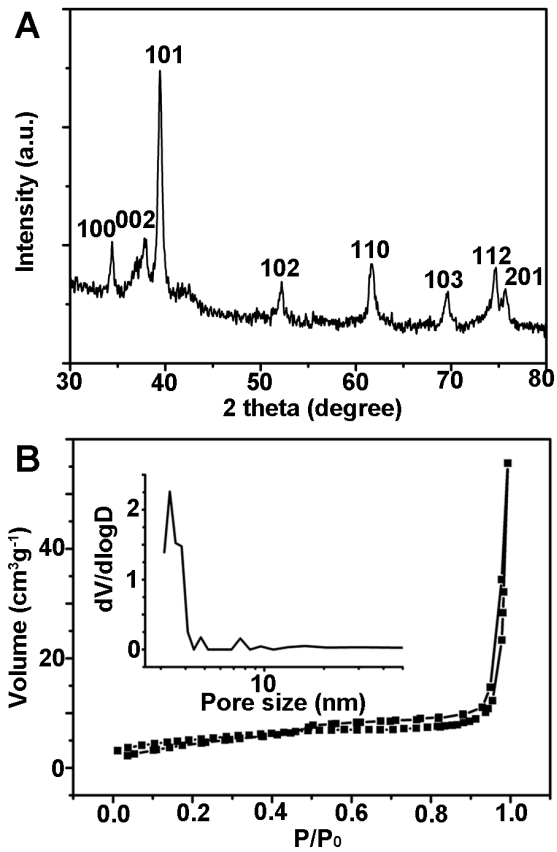


Fig. 2. (A) XRD pattern and (B) N₂ adsorption/desorption isotherm of nano-Mo₂C wires.

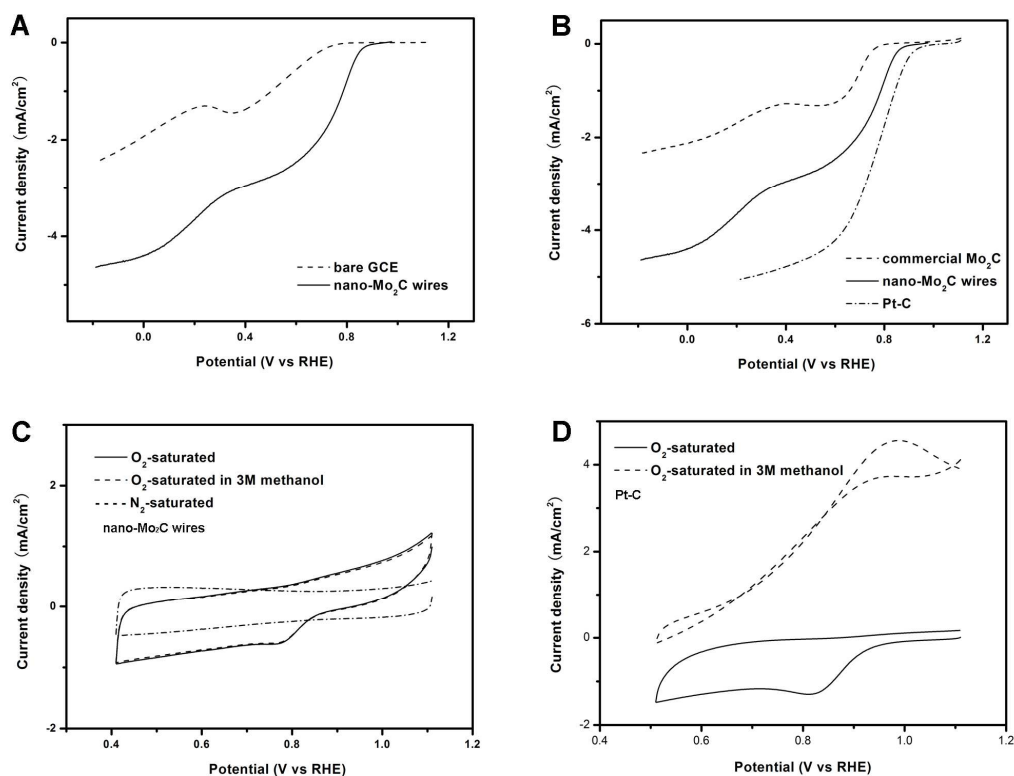


Fig. 3. Polarisation curves of (A) bare and nano-Mo₂C wire modified GC-RDEs and (B) commercial Mo₂C, nano-Mo₂C wire and Pt-C modified GC-RDEs. The LSV experiments were performed with a rotation rate of 1600 rpm, at a scan rate of 10 mV/s, in an oxygen saturated 0.1 M KOH solution. CVs of (C) nano-Mo₂C wires and (D) Pt-C modified GC-RDEs in an oxygen saturated 0.1 M KOH solution, an oxygen saturated 0.1 M KOH solution with the addition of methanol (3.0 M), and a nitrogen saturated 0.1 M KOH solution. Scan rate: 50 mV/s.

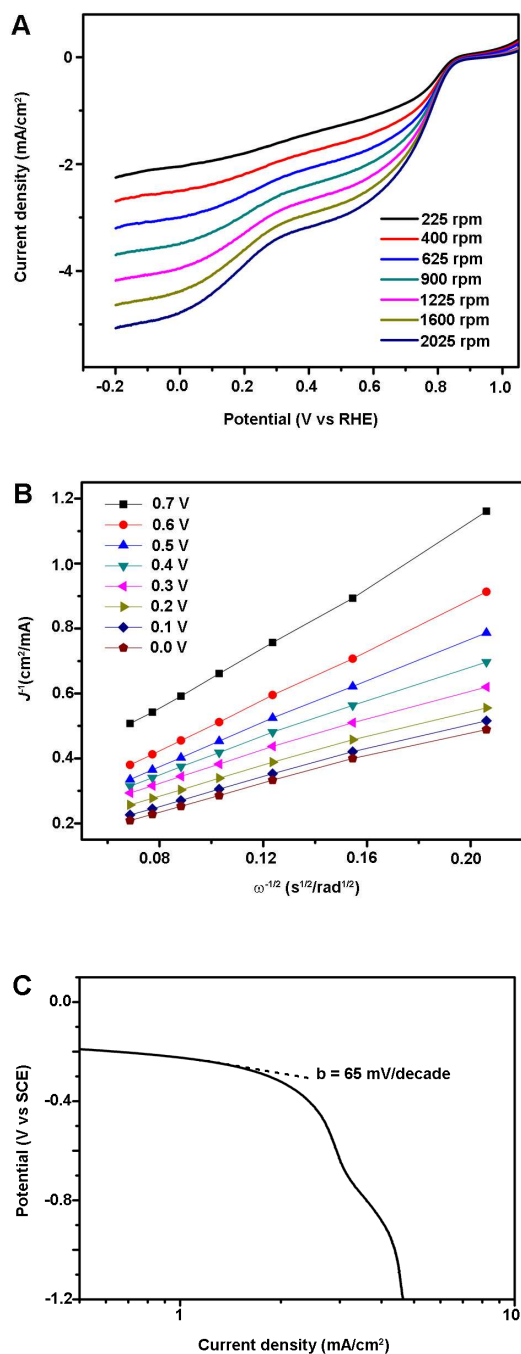


Fig. 4. (A) Polarisation curves of a nano-Mo₂C wire modified GC-RDE with various rotation rates at a scan rate of 10 mV/s in an oxygen saturated 0.1 M KOH solution. (B) The Koutecky-Levich plots of J^{-1} versus $\omega^{-1/2}$ deduced from the data of (A) at different potentials. (C) Tafel plots of nano-Mo₂C derived by the mass-transport correction of the corresponding rotating disk electrode data.

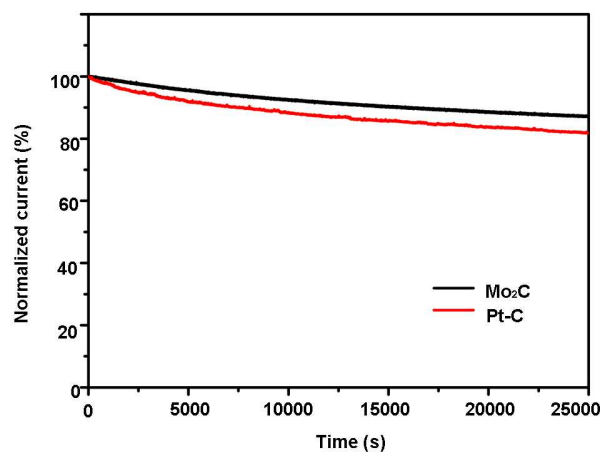


Fig. 5. Chronoamperometric response of nano-Mo₂C wires and Pt-C kept at 0.6 V vs. RHE in an oxygen saturated 0.1 M KOH solution.

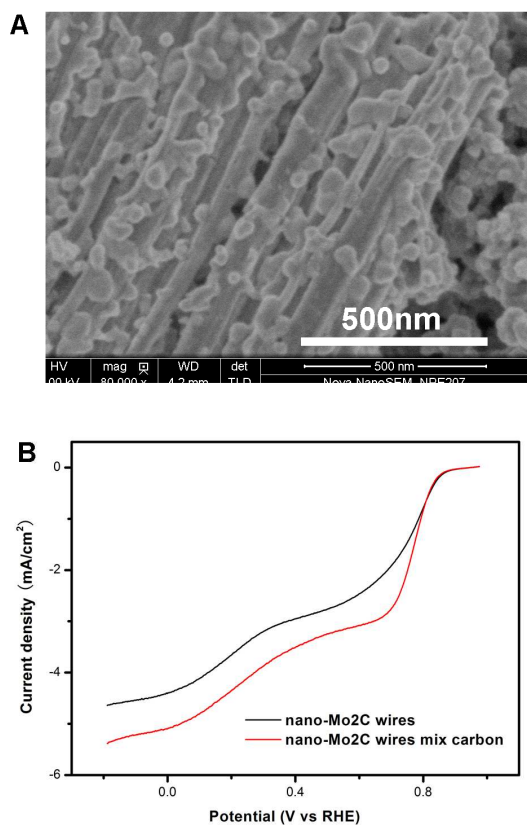


Fig. 6. (A) SEM image of nano Mo₂C wires physically mixed with Vulcan carbon. (B) Polarisation curves of nano-Mo₂C wires, mixed nano-Mo₂C/carbon catalyst modified GC-RDEs with a rotation rate of 1600 rpm, at a scan rate of 10 mV/s, in an oxygen saturated 0.1 M KOH solution.

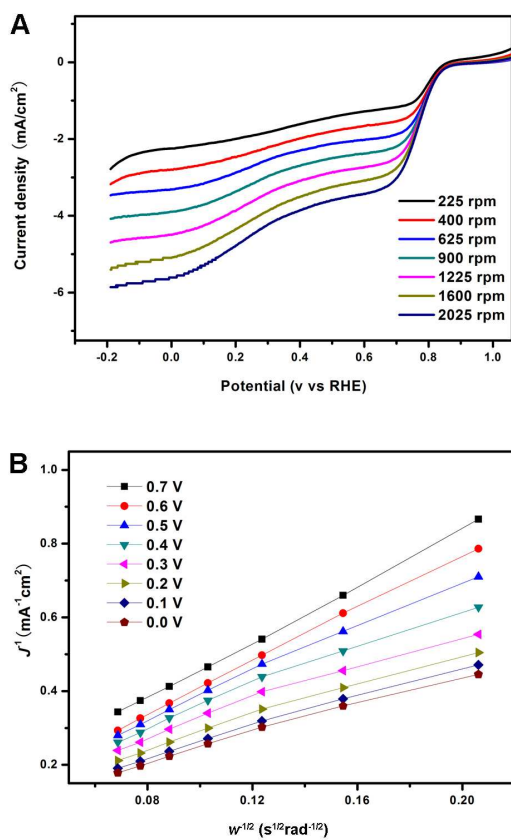


Fig. 7. (A) Polarisation curves of mixed nano-Mo₂C/carbon catalyst modified GC-RDE with various rotation rates at a scan rate of 10 mV/s in an oxygen saturated 0.1 M KOH solution. (B) The Koutecky-Levich plots of J^{-1} versus $\omega^{-1/2}$ deduced from the data of (A) at different potentials.